



## Bearings Health Monitoring Based on Frequency-Domain Vibration Signals Analysis

Saja M. Jawad , Alaa A. Jaber 

Mechanical Engineering Dept., University of Technology-Iraq, Alsina'a street, 10066 Baghdad, Iraq.

\*Corresponding author Email: [20332@uotechnology.edu.iq](mailto:20332@uotechnology.edu.iq)

### HIGHLIGHTS

- Fabricate test rig to simulate the state and capture information
- Extraction time domain signal.
- Transform time domain to frequency domain by FFT transform using sigview program.
- Analysis result.

### ARTICLE INFO

**Handling editor:** Sattar Aljabbair

#### Keywords:

Vibration signal analysis; Bearing fault detection; Time-domain signal analysis; Frequency-domain signal analysis; Fault frequencies.

### ABSTRACT

Rotating machine health monitoring is critical for system safety, cost savings, and increased reliability. The need for a simple and accurate fault diagnosis method has led to the development of various monitoring techniques. They incorporate vibration, motor's current signature, and acoustic emission signals analysis in condition monitoring. So, based on using vibration signal analysis, a test rig was built for bearing fault identification. The test rig replicates and investigates various bearing problems, such as those found in the inner and outer races. An accelerometer, type ADXL335, was interfaced to a data acquisition device (DAQ USB-6215) for collecting vibration signals under various operating circumstances. In addition, a load cell was embedded with the test rig, interfaced with a digital panel meter, and used for recording the applied load on the bearings. The time-domain signal analysis technique was used after acquiring vibration signals at various bearing health states. Then, the time-domain signal was converted to the frequency domain using the fast Fourier transform, and the result was analyzed to investigate the generated fault frequencies. Finally, the obtained frequencies were compared with the theoretical values extracted from the theoretical equations, and the method proved its effectiveness in detecting the fault generated.

## 1. Introduction

In the modern world, rotating machinery is a significant industrial machine. Motors, for example, currently provide almost half of the supplied mechanical energy to different manufacturing activities in the United States [1]. Rolling element bearings are the most meticulously crafted devices; however, they may fail prematurely if worrisome forces are adequate [2]. Any fault in the bearings can harm production and tools and be unsafe. As a result, bearing condition monitoring and fault diagnosis has become a critical research area for industrial advancement [3]. Generally, faults, including the inner and outer races, predominately happen in rolling elements, increasing during bearing running. Therefore, it is crucial to detect and diagnose faults at the premature stages of their initiation [4]. Various equipment condition monitoring methods rely on physical magnitudes like vibration, stator currents, and auditory emission signals. For instance, for condition monitoring of electrical rotating machinery, the stator current signature analysis has been used as it is non-invasive and easy to apply. Because the induction motor's current consumption is governed by mechanical efforts and vibration patterns within the rotational machine, current analysis can reveal the effects of mechanical faults. The acoustic emission (AE) technique has an advantage over vibration analysis and provides earlier identification of issues than oil analysis and other more proven techniques. However, AE signals often contain a large amount of noise, minimizing the possibility of early defect detection [5].

Ball bearings are the most significant used components for supporting and motion transmission components in rotating machinery. In a rotor-bearing system, the bearing outer race is usually fastened to the housing while the bearing inner race spins with the shaft. Thus, bearing loads and vibrations are conveyed from the rotor to the housing via the bearing inner race, balls, and outer race. Furthermore, the cage keeps the balls from slipping and rubbing against one another [6]. Vibration analysis is commonly used to find faults in rotational machines. Various vibration analysis methods have been used to

diagnose rotating machine faults. Some researchers have reviewed the commonly followed vibration analysis techniques from various perspectives.

In the 1980s, Mathew and Alfredo reviewed vibration monitoring techniques for rolling element bearings in the time and frequency domains. Even in healthy running states, machines vibrate because of tiny minor flaws. However, almost all machines have a vibration level that may be considered a standard healthy condition. Usually, the level of vibration in machines increases due to the development of mechanical abnormalities. The vibration level of the machine is measured with the assistance of sensors. Accelerometers are mostly used for vibration analysis—machine fault diagnosis normally has many stages. Firstly, noisy vibration signals are captured utilizing data-gathering equipment. These tainted signals may fail to detect defects. Some approaches can help detect vibrations that otherwise go unreported. After the data gathering step, features from signals can be extracted, and based on the results from analyzing the features, the faults can be detected in the last step [7].

However, this research is a continuation of a previously conducted work published in [8]. As a result, this paper aims to detect bearing faults using vibration analysis based on time- and frequency-domain signals analysis. The following objectives have been established to reach this goal: (1) design and manufacture a test rig to perform the planned experimental work (2) perform a comprehensive analysis of prior studies in the area of bearing health monitoring (3) develop a suitable data acquisition method for recording vibration signals. Then, the captured time-domain vibration signals must be analyzed using the fast Fourier transformation to translate the acquired signal into the frequency domain.

## 1.1 Vibration Signals Analysis Techniques

A wide diversity of techniques utilizing different algorithms was presented to detect and diagnose defects in rolling element bearings, which have been introduced to test raw vibration signals [9]. Vibration monitoring is the most popular approach to detect abnormalities in rolling bearings since it is precise and sensitive to the severity of the faults. However, defects in bearing components serve as a source of vibration and noise. Therefore, the information contained in these vibration signals will assist us in determining the current condition of the bearing [10]. The commonly followed vibration signals analysis algorithms are classified according to their domain of operation into time, frequency, or time-frequency domains.

### 1.1.1 Time domain technique

The approach of analyzing time-domain data is usually used to monitor the health status of different mechanical components. It is based on extracting certain statistical characteristics such as the root mean square (RMS), kurtosis, crest factor, skewness, and peak-to-peak values [11].

### 1.1.2 Frequency domain technique

The frequency-domain or spectrum analysis technique is the most extensively used methodology for bearing defect diagnostics. Using the fast Fourier transform, the frequency-domain signal analysis methodology turns time-domain vibration data into discrete frequency components (FFT) [12]. The frequency is represented on the X-axis, while the amplitude is represented on the Y-axis in a frequency spectrum plot. As a result, the frequency-domain technique is superior to the time-domain technique in detecting certain frequency components [13].

### 1.1.3 Time-frequency domain analysis

Signals generated by faulty parts are non-stationary. When the Fourier transform is employed to obtain the frequency variables of the non-stationary signals, the frequency composition is averaged across the signal's duration. As a result, the Fourier transform cannot adequately capture the features of a transitory signal; however, time-frequency analysis has been researched and employed for machinery failure diagnostics due to its capacity to represent the signals in both the frequency and time domains. Time-frequency analysis techniques are useful for non-stationary data because of this unique property. Additionally, time-frequency approaches may be advantageous for determining energy distribution across frequency bands. Numerous time-frequency analysis approaches have been used to discover and diagnose problems, including the short-time Fourier transform (STFT), the wavelet transforms (WT), the wavelet packet transform (WPT), and the Hilbert-Huang transform (HHT) [14].

## 1.2 Characteristic Defect Frequencies

An impulsive vibration is produced when a flaw appears on any bearing element, known as fault frequency. The frequency is determined by the location of the fault and the shaft's rotational speed. The common frequencies generated in rolling element bearings are the fundamental train frequency (FTF), ball pass frequency of inner race (BPF<sub>I</sub>), ball pass frequency of outer race (BPF<sub>O</sub>), and ball spin frequency (BSF). They were calculated using the below equations [15]. The common rolling element bearings geometry consists of four components: the outer race, inner race, ball, and cage involved in producing the fault frequencies [3].

Fundamental cage frequency

$$FTF = \frac{f_s}{2} \left( 1 - \frac{d}{D} \cos \alpha \right) \quad (1)$$

Ball defect frequency

$$BSF = \frac{D f_s}{2d} \left( 1 - \frac{d^2}{D^2} \cos^2(\alpha) \right) \quad (2)$$

Inner race defect frequency

$$BPFI = \frac{n_b f_s}{2} \left( 1 + \frac{d}{D} \cos \alpha \right) \quad (3)$$

Outer race defect frequency-

$$BPFO = \frac{n_b f_s}{2} \left( 1 - \frac{d}{D} \cos \alpha \right) \quad (4)$$

The shaft rotation frequency ( $f_s$ ), the number of rollers ( $n_b$ ), the ball diameter ( $d$ ), the bearing pitch diameter ( $D$ ), and the contact angle ( $\alpha$ ) are all included in these calculations [16].

## 2. Experimental Procedure

### 2.1 Test Rig Design and Development

The test rig aims to obtain a full-scale platform capable of performing the required tests on bearings in different stages of health. A frame, a 1 HP (0.75 kW) AC motor, pulleys (driver attached to the motor and driven attached to shaft via key and seal), a belt, and a mild steel shaft with a diameter of 20 mm comprise the rig's essential components. The bearings are supported on two identical deep groove ball bearings installed in two cast iron housings. The information in Table 1 pertains to the ball bearing that was utilized. Figure 1 illustrates a SolidWorks model of the proposed design for the test rig [17].

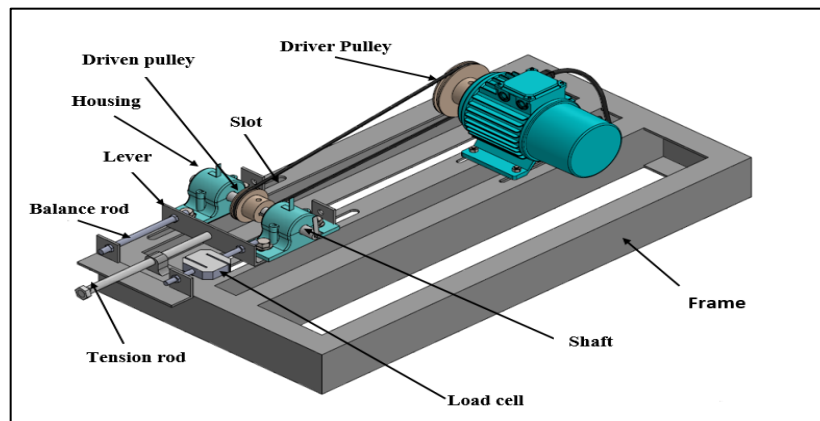


Figure 1: Solid work model of the suggested test rig design

Table 1: 6304 Ball bearing specification

| Number. Of balls( $N_b$ ) | 7        |
|---------------------------|----------|
| Inner diameter            | 20(mm)   |
| Outer diameter            | 52(mm)   |
| Bearing contact angle     | 0        |
| Ball diameter             | 9.53(mm) |
| Pitch diameter            | 36(mm)   |

A simple mechanism was used to apply the load, which moved the bearing housing on the base. This was accomplished by inserting a steel plate (lever) through a slot in the rig's base between the bearing housing and the rig's base. This device can draw the bearing housing and shaft together using the pulley and belt, imposing a force on the shaft. This force can be varied by modifying the tension rod's pulling force to pull the system easily. In addition, a slot under the motor was created to boost the test rig's flexibility by allowing linear movement to increase or decrease the load on the shaft and the bearings. Figure 2 depicts the completed test rig.

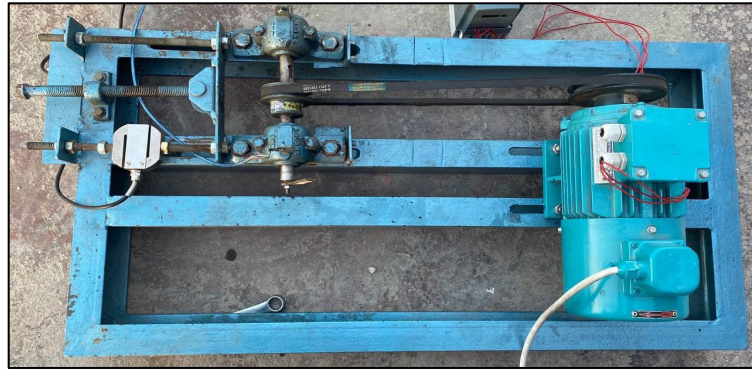


Figure 2: The fabricated test rig

A seal was drilled on the shaft using a CNC machine to fix the pulley on the shaft. A key was used between the shaft and pulley. A U-section channel with a thickness of 6 mm was chosen for its weight and capacity to support the construction when taking readings and preventing undesired vibrations. The system has been stabilized by placing four rubber pieces under the structure. The induction motor utilized has a fixed speed; however, a variable frequency drive (VFD) of Hyundai's type N700E inverter was used to vary the rotation speed to simulate varying working speeds on the system. An ADXL335 accelerometer was attached to the left bearing and used in conjunction with a rectangular steel adaptor to detect vibration. A screw held the accelerometer firmly in place on the bearing housing. A laser tachometer was also used to measure the shaft's speed. However, due to the small diameter of the shaft, it was not easy to place the adhesive tape on it to measure the speed; therefore, a steel piece was connected to the shaft, and the tape was placed on it, as shown in Figure 3.



Figure 3: Method of speed measurement

## 2.2 Bearing Faults Simulation

Four different fault types are seeded in the bearing: an inner race fault, an outer race fault, a combined cage and ball fault, and an inner and outer race fault combined with another defect. Electrical discharge machining (EDM) was used to create these faults. It is a technique for eliminating metal and is typically utilized to work with exceptionally hard materials or tough to process with traditional methods. It can only be used on electrically conductive materials. A strong current is passed between an electrode and the component in an electrolytic material removal procedure that uses a negatively charged electrode (cathode), a conductive fluid (electrolyte), and a conductive workpiece (anode). The outer and inner races of the defect have a diameter of 3.2 mm. When the outer race malfunctioned, the electrode was put vertically in the machine, whereas the inner race fault was created by rotating the electrode end 90 degrees. As a result, the length of the turned part was 10 mm, and the ball bearing was fixed horizontally, as shown in Figure 4. Researchers compare faulty and healthy cases to understand bearing vibration behavior when a fault develops in one of its components. Figure 5 depicts the four simulated faults in the bearings [18].



Figure 4: Inner race fault simulation method



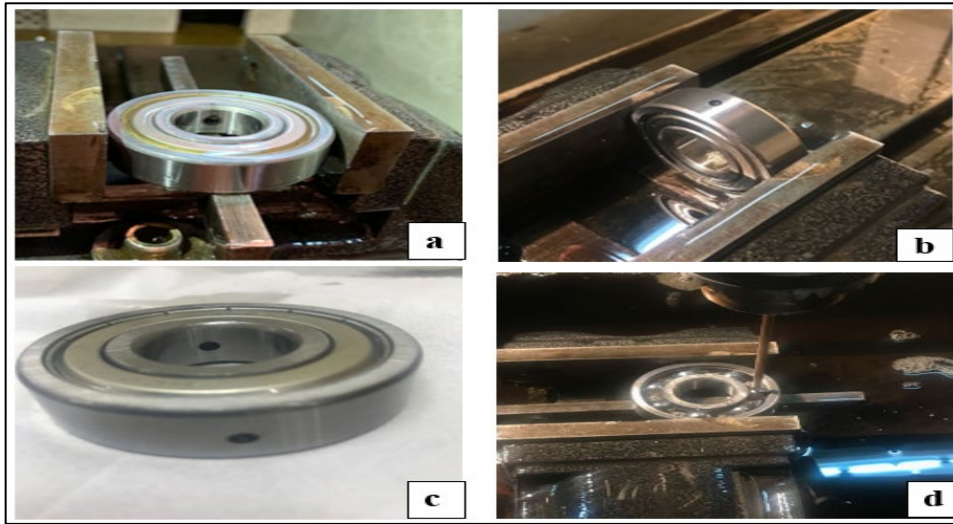


Figure 5: Types of the simulated faults (a) Inner race fault, (b) Outer race fault, (c) Combined inner and outer race fault, and (d) Combined cage and ball fault

Vibration analysis was used to investigate the impact of these faults on the designed test rig. Results from 30 trials at various rotating speeds and under various loading circumstances were analyzed. Table 2 displays the results of the 30 different test scenarios that were run.

Table 2: The accomplished experimental scenarios on the bearing

| Load | Healthy bearing | Inner race fault | Outer race fault | Combined Cage and ball fault | Combined Inner and outer race fault |
|------|-----------------|------------------|------------------|------------------------------|-------------------------------------|
| 25kg |                 |                  |                  | 1000 RPM                     |                                     |
|      |                 |                  |                  | 1500 RPM                     |                                     |
|      |                 |                  |                  | 2000 RPM                     |                                     |
| 50kg |                 |                  |                  | 1000 RPM                     |                                     |
|      |                 |                  |                  | 1500 RPM                     |                                     |
|      |                 |                  |                  | 2000 RPM                     |                                     |

### 2.3 The Developed Data Acquisition System

Vibration signals must be gathered and examined to monitor the operating state of the bearing under investigation to see whether there is anything wrong with its health. Vibration data is collected by an accelerometer. The acquired signals are then sent to a computer running a customized LabView application that analyzes them. Finally, the system's applied load can be determined utilizing a load cell sensor directly attached to a Digital Panel Meter that displays the amount of the applied force.

### 2.4 Test Rig Final Set-Up

The accelerometer is placed on the first bearing and interfaced to the data-collecting computer via a cable. Next, the load cell is properly positioned, as shown in Figure 6, and interfaced to the digital panel meter, which shows load values immediately and after the electrical motor is turned on and off. As a result, the motor is linked to the alternating current drive, which is subsequently connected to the electrical socket, allowing for variable speed operation. Last, the device is started at the specified speed, and the force is applied to the specified shaft. The preceding procedures must be repeated each time a simulated ball-bearing defect is changed. Data from the accelerometer is collected continuously using the built-in LabVIEW program, which allows for data viewing and analysis and data saving to Excel spreadsheets.

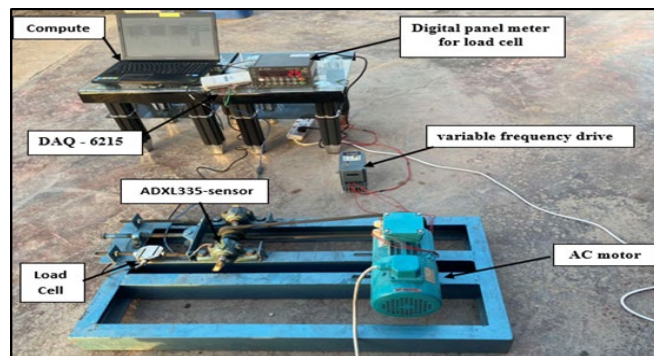


Figure 6: Test rig final set-up

### 3. Results and Discussion

#### 3.1 Studying The Effect of Applied Load

The test rig was rotated at a constant rotational speed. At the same time, the applied load was increased progressively to explore the effect of loading circumstances on the fluctuation of the vibration signal when the bearing is healthy and faulty (inner, outer race, combined inner and outer, and ball and cage faults). In Figure 7, an increase in the applied load results in a modest increase in the acceleration amplitude. This is because increasing the applied load places pressure on the system, increasing the vibration amplitudes. Noting that the combined fault (ball and cage) is more susceptible to damage than the other fault kinds. It is possible that the ball and cage fault results in a greater vibration amplitude, making this type of damage more harmful than the others

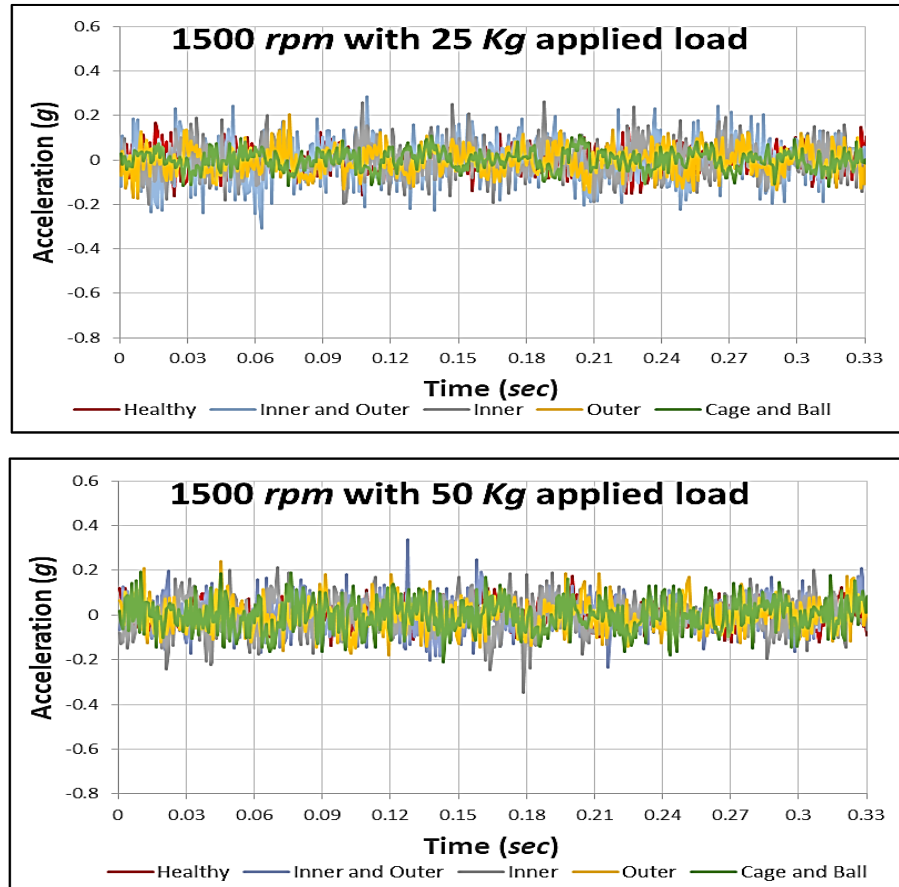


Figure 7: Time-domain signals of the five bearing's health states at 1500 rpm with different applied loads

#### 3.2 Studying the Effect of Rotating Speed

From Figure 8, it can be noticed that the acceleration increases as the rotational speed increases. This is because increasing the rotation speed leads to an increase in the centrifugal forces. In addition, the increase in the amplitude of the combined fault cases (inner and outer races fault and ball and cage fault) is more than the other fault types. This is due to the severity of the simulated faults, which produce intensive pulses as the speed increases leading to exciting the system resonance frequencies. From this, it can be concluded that the combined defects are more serious, more sensitive to the rotation speed, and has a greater effect on the overall vibration level of the rotating systems.

#### 3.3 Frequency Domain Analysis

Time-domain signals can be transformed into frequency-domain signals using a fast Fourier transform (FFT). On the other hand, the obtained frequency domain signal is referred to as a vibration signature/response or a frequency spectrum. Using SIGVIEW software, a real-time signal analysis application was performed. It included spectral analysis tools, statistical functions, and comprehensive graphical solutions for 2D and 3D graphics. The captured time-domain vibration signals were converted into frequency domain signals using fast Fourier transforms (FFT). It can produce a clear graphical representation between the amplitudes and frequencies for easy signal analysis by examining the differences in vibration amplitudes due to the various operating conditions.

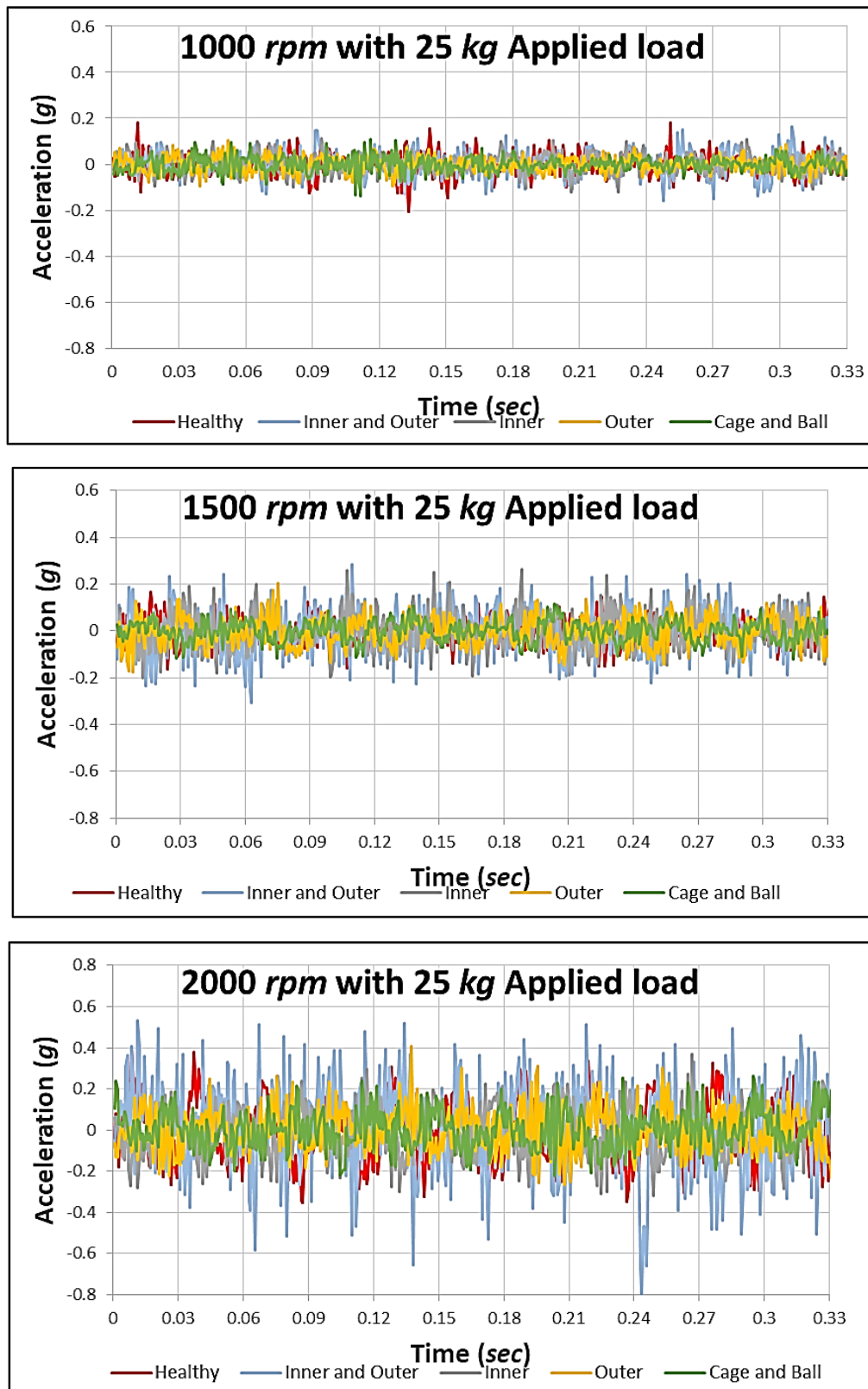


**Figure 8:** Time-domain signals from the five bearing health conditions at 25 Kg at different rotating speeds

The vibration signal response is obtained at 1500 rpm and 50 Kg load for the testing bearing, as shown in Figure 9. The operating frequency, which is referred to as  $1X = 25$  Hz, and its multipliers/harmonics, which are referred to as  $2X$ ,  $3X$ ,  $4X$ , etc., can clearly be observed in the frequency spectrum of the captured vibration signal of the tested faulty bearings when they are compared with the spectrum of healthy bearings under the same operation conditions (see Figure 9). The theoretical fault frequencies can be computed using Equations 1-4, as shown in Table 3. The amplitudes at  $1X$  and its harmonics in the faulty bearing are higher than the healthy bearing in the vibration signal spectrum.

The evident high peaks in Figure 9 have been indicated and analyzed. For example, Figure 9A shows that the amplitudes are high at frequencies referred to as multiples of the operating frequency in the healthy bearing case. While in the case of the

inner race fault, Figure 9B, the operating frequency and its multiples are also shown with higher amplitudes than in the healthy case. The inner race fault frequency (BPFI), which is 110.66 Hz (obtained based on Equation 3), and its multiples can be easily noted. The vibration amplitude at the experimental inner fault frequency of 114 Hz is clearly shown in Figure 9B. In the case of the outer race fault (Figure 9C), high peaks can be detected; they are either multiple of the operating frequency or the frequency of the calculated outer race fault (BPFO), which is 64.33 Hz obtained based on Equation 4.

For the case of a combined fault (defects in the inner and outer races), the frequency spectrum is shown in Figure 9D. Higher peaks can be detected at frequencies either multiple of the operating frequency or related to the obtained frequencies of the outer race fault (BPFO), inner race fault (BPFI), or one of their multiples. However, Figure 9E shows the frequency spectrum of the case of the combined fault (cage and ball fault). The significant amplitudes represent either multiple of the operating frequency or the obtained cage fault frequency (FTF) or ball fault frequency (BSF), which are 9.19 Hz and 43.91 Hz, respectively, or their multiples.

**Table 3:** Theoretical fault frequencies

| RPM  | Hz<br><i>Operation frequency</i> | Fault Frequencies Calculated Theoretically |             |            |            |
|------|----------------------------------|--|-------------|------------|------------|
|      |                                  | <i>BPFI</i>                                | <i>BPFO</i> | <i>BSF</i> | <i>FTF</i> |
| 1000 | 16.66                            | 73.74                                      | 42.87       | 29.26      | 6.124      |
| 1500 | 25                               | 110.66                                     | 64.33       | 43.91      | 9.19       |
| 2000 | 33.33                            | 147.53                                     | 85.77       | 58.54      | 12.25      |

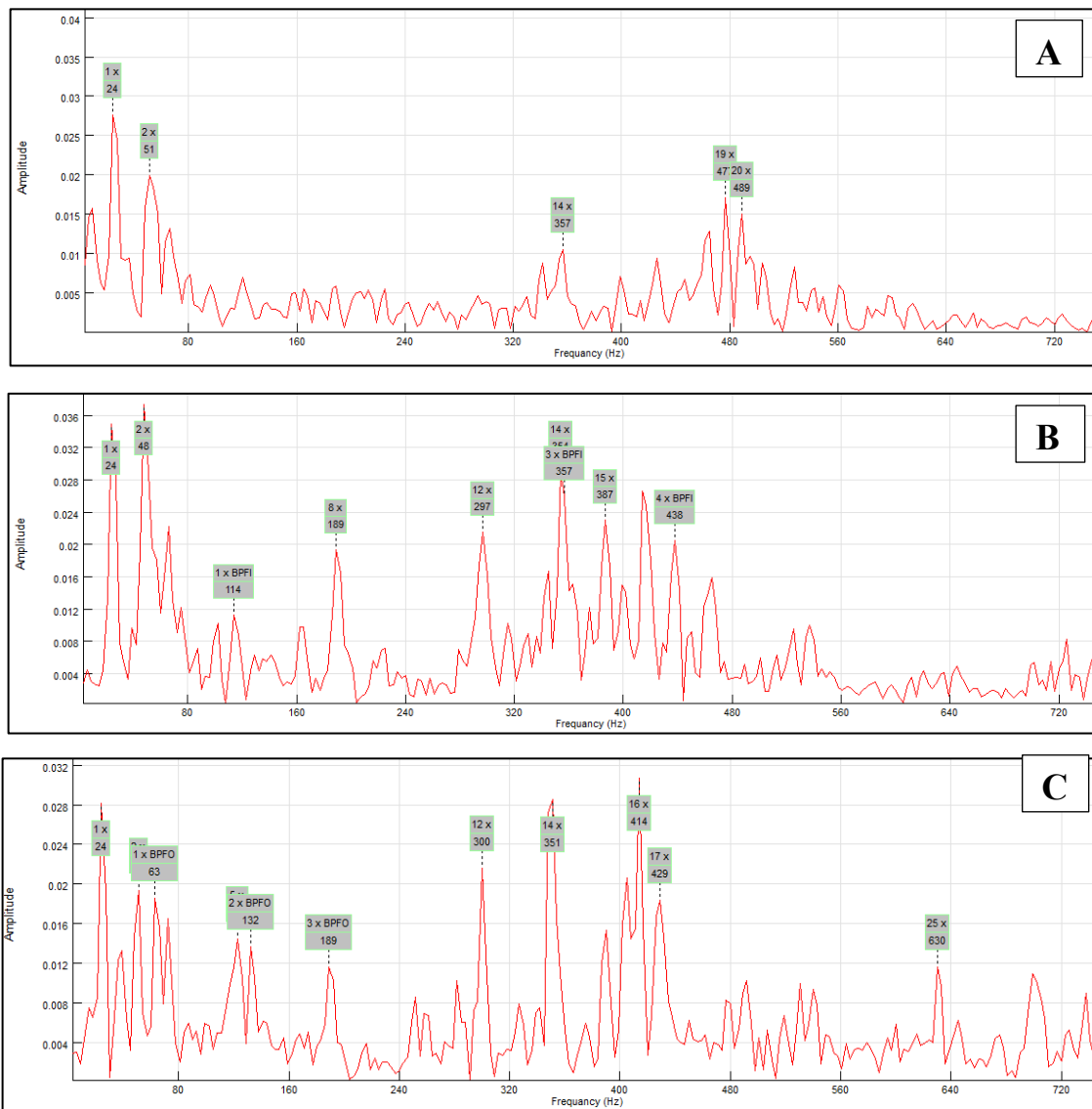


**Figure 9:** Vibration signal spectrum at 25 Hz with 50 Kg applied load, (A) healthy bearing, (B) inner race fault, (C) outer race fault, (D) combined inner and outer race faults, and (E) cage and ball faults



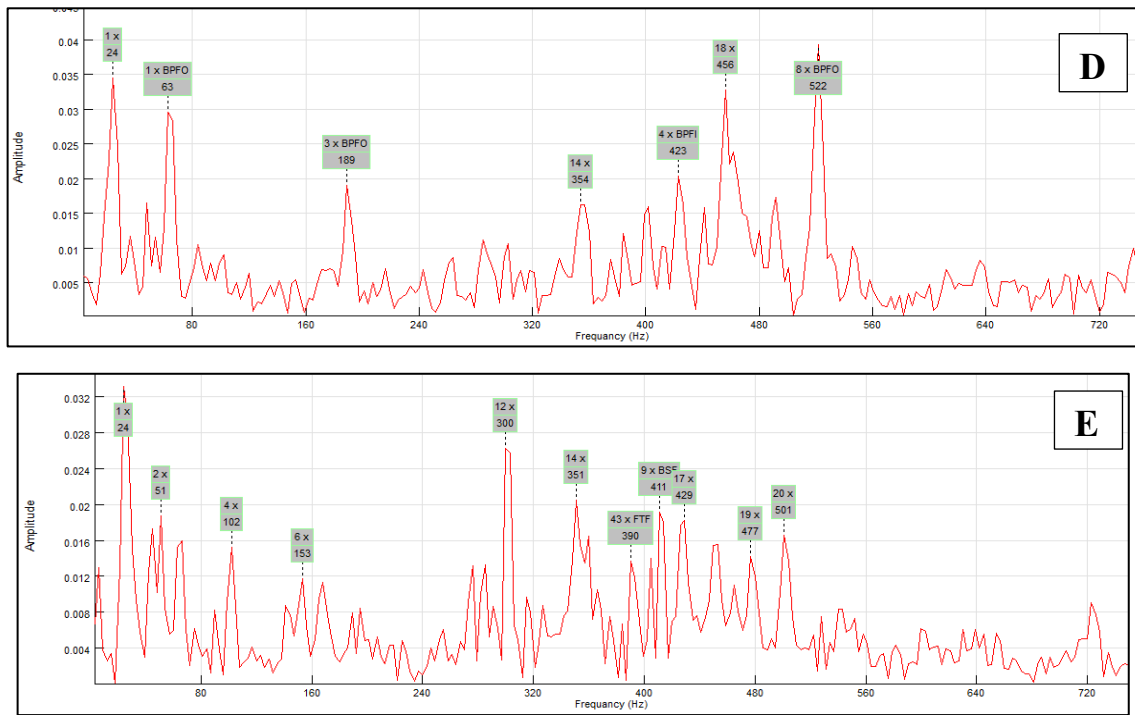


Figure 9: Continued

#### 4. Conclusions

This study constructed an experimental test rig to assess the bearing defect detection method based on vibration signal analysis. Numerous experiments were undertaken to determine the effect of varying bearing health on the intensity of machine vibration. The simulated bearing faults were an inner race fault, an outer race fault, a combination of inner and outer race fault, and a ball and cage fault. An instrument from National Instruments was used to collect the vibration signals, a data collection system built based on the NI 6215 DQA and LabVIEW software. The bearing was subjected to various rotational speeds and loads while vibrations were recorded. Vibration-based condition monitoring can detect bearing flaws by monitoring time-domain signals. The impact of the bearing fault varies with rotation speed and load.

Notably, the vibration signal spectrum can reveal bearing defects. The fast Fourier transform can be used to investigate the frequency spectrum. The feature amplitudes are modest when the bearing is healthy but highest when simulated faults. Because the ball always collides with the simulated damage when the inner race rotates with the shaft, high vibration amplitudes ensue. As a result, the combined flaws (inner/outer race flaws, cage/ball flaws) affect the rotating system's overall vibration level. The combined fault instance has two faults functioning simultaneously, resulting in the greatest vibration amplitudes. As a result, vibration intensity increases with rotation speed and applied load. It was also shown that the combined ball and cage fault is more sensitive than other faults, meaning that the ball or cage defect produces bearing damage faster than other faults. An intelligent system based on machine learning methodologies, such as artificial neural networks, is proposed for future work to diagnose various bearing faults.

#### Author contribution

All authors contributed equally to this work.

#### Funding

This research received no specific grant from any funding agency in the public, commercial, or not-for-profit sectors.

#### Data availability statement

The information was taken by the researcher, and the rest of the data is in the author's thesis in the Department of Mechanical Engineering, University of Technology library.

#### Conflicts of interest

The authors declare that there is no conflict of interest.

#### References

- [1] X. Jin, M. Zhao, T. W. Chow, M. Pecht, Motor bearing fault diagnosis using trace ratio linear discriminant analysis, IEEE Trans. Ind. Electron., 61 (2014) 2441-2451. <https://doi.org/10.1109/TIE.2013.2273471>

- [2] D. S. Chandra, Y. S. Rao, Fault Diagnosis of a Double-Row Spherical Roller Bearing for Induction Motor Using Vibration Monitoring Technique, *J. Fail. Anal. Prev.*, 19 (2019) 1144-1152. <https://doi.org/10.1007/s11668-019-00712-z>
- [3] A. Boudiaf, A. Moussaoui, A. Dahane, I. Atoui, A comparative study of various methods of bearing faults diagnosis using the case Western Reserve University data, *J. Fail. Anal. Prev.*, 16 (2016) 271-284. <https://doi.org/10.1007/s11668-016-0080-7>
- [4] S. Fu, K. Liu, Y. Xu, Y. Liu, Rolling bearing diagnosing method based on time domain analysis and adaptive fuzzy-means clustering, *Shock Vib.*, 2016 (2016). <https://doi.org/10.1155/2016/9412787>
- [5] J. J. Saucedo-Dorantes, M. Delgado-Prieto, J. A. Ortega-Redondo, R. A. Osornio-Rios, R. d. J. Romero-Troncoso, Multiple-fault detection methodology based on vibration and current analysis applied to bearings in induction motors and gearboxes on the kinematic chain, *Shock Vib.* 2016 (2016). <https://doi.org/10.1155/2016/5467643>
- [6] F. Bin, Z. Jinhua, Y. Ke, H. Jun, Y. W. Michael, A comprehensive study on the speed-varying stiffness of ball bearing under different load conditions, *Mech. Mach. Theory*, 136 (2019) 1-13. <https://doi.org/10.1016/j.mechmachtheory.2019.02.012>
- [7] M. Vishwakarma, R. Purohit, V. Harshlata, P. Rajput, Vibration analysis & condition monitoring for rotating machines: a review, *Mater. Today Proc.*, 4 (2017) 2659-2664. <https://doi.org/10.1016/j.matpr.2017.02.140>
- [8] S. M. Jawad, A. Jaber, Rolling Bearing Fault Detection Based on Vibration Signal Analysis and Cumulative Sum Control Chart, *FME Transactions*, 49 (2021) 684-695. <https://doi.org/10.5937/fme2103684M>
- [9] J. Chebil, M. Hrairi, N. Abushikhah, Signal analysis of vibration measurements for condition monitoring of bearings, *Aust. J. Basic Appl. Sci.*, 5 (2011).
- [10] S. Patidar, P. K. Soni, An overview on vibration analysis techniques for the diagnosis of rolling element bearing faults, *Int. J. Eng. Trends Technol.*, 4 (2013) 1804-1809.
- [11] P. R. Manve, R. S. Narasimha, condition monitoring and fault identification of new deep groove ball bearing using labview, *J. Emerg. Technol. Innov. Res.*, 4 (2017) 104-108.
- [12] H. Musbah, M. El-Hawary, SARIMA Model Forecasting of Short-Term Electrical Load Data Augmented by Fast Fourier Transform Seasonality Detection, *IEEE Can. Conf. Electr. Comput. Eng.*, Edmonton, AB, Canada, (2019) 1-4. <https://doi.org/10.1109/CCECE.2019.8861542>
- [13] P. Gupta, M. Pradhan, Fault detection analysis in rolling element bearing: A review, *Mater. Today Proceedings*, 4 (2017) 2085-2094. <https://doi.org/10.1016/j.matpr.2017.02.054>
- [14] Z. Xia, S. Xia, L. Wan, S. Cai, Spectral regression based fault feature extraction for bearing accelerometer sensor signals, *Sensors*, 12 (2012) 13694-13719. <https://doi.org/10.3390/s121013694>
- [15] M. M. Tahir, S. Badshah, A. Hussain, M. A. Khattak, Extracting accurate time domain features from vibration signals for reliable classification of bearing faults, *Int. J. Adv. Appl. Sci.*, 5 (2018) 156-163. <https://doi.org/10.21833/ijaas.2018.01.021>
- [16] D. S. J. Lacey, An Overview of Bearing Vibration Analysis, *InA&FAG*, 2008
- [17] S. M. Jawad, A. A. Jaber, Rolling bearing fault detection based on vibration signal analysis and cumulative sum control chart, *FME Transactions*, 49 (2021) 684-695. <https://doi.org/10.5937/fme2103684M>
- [18] C. J. Yuan, A. S. H. A. Bakar, M. N. Roslan, C. W. Cheng, M. N. S. M. Rosekhizam, J. A. Ghani, et al., Electrochemical machining (ECM) and its recent development, *J. Tribol.*, 28 (2021) 20-31.